ACS APPLIED MATERIALS & INTERFACES

Research Article

www.acsami.org

Composite PLGA/AgNpPGA/AscH Nanospheres with Combined Osteoinductive, Antioxidative, and Antimicrobial Activities

Magdalena Stevanović,*[,†] Vuk Uskoković,[‡] Miloš Filipović,[§] Srečo D. Škapin,[∥] and Dragan Uskoković[†]

[†]Institute of Technical Sciences of the Serbian Academy of Sciences and Arts, 11000 Belgrade, Serbia

[‡]Therapeutic Micro and Nanotechnology Laboratory, Department of Bioengineering and Therapeutic Sciences, University of California, San Francisco, California 94158, United States

[§]Department of Chemistry and Pharmacy, University of Erlangen-Nuremberg, 91058 Erlangen, Germany

[∥]Advanced Materials Department, Jožef Štefan Institute, Ljubljana, 1000, Slovenia

Supporting Information

ABSTRACT: The global rise in the resistance of pathogens to conventional antibiotics has created an intensive search for alternative materials with antimicrobial properties. This study is performed with an intention to investigate the combined effects of poly(L-glutamic acid)-capped silver nanoparticles (AgNpPGA) and ascorbic acid (AscH) encapsulated within freeze-dried poly(lactide-co-glycolide) (PLGA) nanospheres to obtain a nanomaterial with simultaneous osteoinductive, antioxidative, and prolonged antimicrobial properties. The influence of PLGA/AgNpPGA/AscH particles on (i) viability and superoxide production of human umbilical vein endothelial cells in vitro, (ii) morphology and expression of osteogenic markers in osteoblastic MC3T3-E1 cells in vitro, and (iii) antimicrobial activity against a Gram-positive bacterium, methicillin-resistant *Staphylococcus aureus*, and a Gram-negative bacterium, *Escherichia coli*, was investigated. PLGA/AgNpPGA/AscH nanoparticles showed a superior and extended antibacterial activity against both types of bacteria. The nanoparticles appeared to be capable of delivering ascorbate to the cells, which was evidenced by the significant decrease in the level of superoxides in human umbilical vein endothelial cells and which could have a therapeutic potential in preventing oxidative stress. PLGA/AgNpPGA/AscH nanoparticles had a positive effect on MC3T3-E1 osteoblastic cells in vitro, promoting: (i) an intimate contact with the cells and preservation of their healthy morphologies; (ii) unreduced cell viability; and (iii) multiple-fold upregulation of two osteogenic markers: osteocalcin and type I procollagen. It is concluded that PLGA/AgNpPGA/AscH nanospheres present a promising new material for the treatment of infections and use in wound dressings and other prophylactic applications.

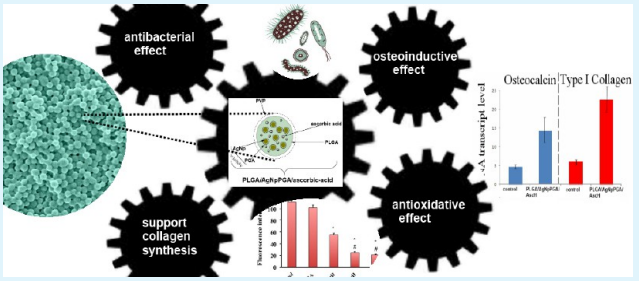

KEYWORDS: *nanotechnology, PLGA, silver nanoparticles, osteoinductivity, antibacterial material, antioxidative effects*

INTRODUCTION

Medical devices are significant risk factors for nosocomial infections, a.k.a. hospital-acquired infections, not present nor incubating at admission.[1−3] These infections are widespread and are important contributors to hospital morbidity. The most common hospital-acquired infections include those of surgical wounds, bloodstream, lower respiratory tract, skin, and urinary tract.[4] Many different microorganisms may cause them. For example, the Gram-positive bacterium *Staphylococcus aureus* causes a variety of lung, bone, heart, and bloodstream infections. Gram-negative bacteria, such as Enterobacteriaceae (e.g., *Escherichia coli*, Klebsiella, etc.), may colonize sites due to weakened host defenses (catheter insertion, cannula insertion, etc.) and elicit a variety of disease states consequential to infection.[1−5] Both of these types of infections may be highly resistant to traditional antibiotic therapies. In fact, the global rise in the resistance of pathogens to conventional antibiotics has created an intensive search for alternative materials with antimicrobial properties. Metallic nanoparticles, e.g., silver, gold, and platinum, count as some of the most promising of these alternative inorganic materials with antibacterial and antiviral properties.[6−8] They have been used in an effort to reduce the scope of infection, though in many cases with rather unsatisfactory clinical outcomes.[9]

Due to their large surface-to-weight ratio, nanoparticles exhibit higher solubility, physicochemical reactivity, and antimicrobial activity when compared to conventional preparations. However, metallic nanoparticles might cause diverse side effects, primarily related to the induced production of reactive oxygen species (ROS), known for their ability to damage various cellular organelles and disrupt the normal cell and tissue physiology.[8] A disequilibrium between the formation of reactive oxygen species

Received: June 9, 2013
Accepted: August 28, 2013
Published: August 28, 2013

   dx.doi.org/10.1021/am402237g | ACS Appl. Mater. Interfaces 2013, 5, 9034−9042

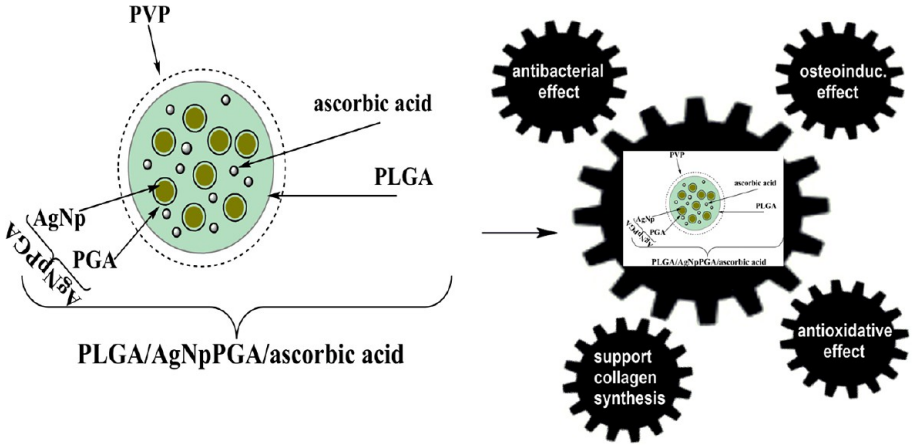

Figure 1. Scheme that illustrates the multifunctional PLGA particle with encapsulated ascorbic acid and PGA-capped silver nanoparticles.

and the defensive, antioxidant molecular species has been involved in the pathogenesis of a variety of ailments, such as respiratory diseases, cancer, diabetes, and cardiovascular and neurodegenerative diseases.[8,10] Synergism of two or more drug combinations increasingly attracts attention as a promising approach to overcome the adverse side effects that limit the clinical applicability of many potential drugs.[11] Therefore, it is of vital significance to devise a co-delivery system that would enable loading of two or more drugs at the same time and transportation to one or multiple target sites. During the last few decades, polymers comprising lactic and glycolic acids and their copolymers have attracted interest as prospective drug delivery carriers in pharmaceutics and tissue engineering.[12,13] Poly(lactide-co-glycolide) (PLGA) is made from two monomers: lactide (diester of lactic acid) and glycolide (diester of glycolic acid), both of which are biocompatible, biodegradable, and nontoxic, in surgical and in drug delivery systems alike.[14] Optimization of the properties of particles, in respect to their most favored interfaces with cells, is of the utmost importance for the biomedical community, being at the same time a major challenge in the field of biomaterials. Common methods to produce PLGA micro- and nanospheres include the emulsification−solvent−evaporation technique (modification of this method is dual or multiple emulsion technique), emulsification−solvent−extraction, and phase separation.[15] In comparison with these methods, the physicochemical solvent/nonsolvent method with freeze drying is a relatively simple, reproducible, rapid, and easily scalable technique. Recently, we have synthesised PLGA microspheres loaded with polyglutamic acid (PGA) capped silver nanoparticles (AgNpPGA)[16] using the physicochemical solvent/nonsolvent technique.[17] We have demonstrated in vitro that the toxicity of bare silver nanoparticles (AgNps) can be reduced: (i) by capping these nanoparticles with an organic layer, i.e., by coating with poly(L-glutamic acid) (AgNpPGAs) and (ii) by their encapsulation (incorporation) within a PLGA polymeric matrix (PLGA/AgNpPGAs). Also, we have shown that these PLGA/AgNpPGA particles can achieve bacterial inhibition levels higher than AgNps or AgNpPGAs.[17]

The purpose of this study has been to combine the freeze-drying method with the physicochemical solvent/nonsolvent approach in the preparation of multifunctional PLGA nanospheres encapsulating AgNpPGA and the common antioxidant, ascorbic acid (vitamin C, AscH). The next aim was to assess its potential not only as an antibacterial material but also as one with pronounced antioxidative properties. In addition, we examined the osteoinductive potential of PLGA/AgNpPGA/AscH nanospheres in vitro.

EXPERIMENTAL SECTION

Freeze-Drying Preparation and Characterization of PLGA/AgNpPGA/AscH Nanospheres. Details about chemicals used for the synthesis of PLGA/AgNpPGA/AscH nanospheres are provided within the Supporting Information (SI).

PLGA/AgNpPGA/AscH nanospheres were produced using a combination of the physicochemical solvent/nonsolvent method and freeze drying. First off all AgNpPGAs were prepared in our laboratory as described in previous reports[16,18] (a procedure of obtaining AgNpPGAs is described in the SI). Then, the solution containing AgNpPGAs was added to an aqueous solution of ascorbic acid (0.1 wt %), continuously being homogenized at 300 rpm during 20 minutes, with the resulting solution becoming grayish green. The volume ratio between the solution containing silver nanoparticles and the solution containing ascorbic acid was 1:3. Additionally, such an obtained mixture of AgNpPGAs and ascorbic acid was encapsulated within the PLGA matrix (Figure 1). AgNpPGA/ascorbic acid was added dropwise to PLGA solution in acetone (120 mg in 20 mL). Afterwards 22 mL of ethanol as nonsolvent was added, and at that instant, after the diffusion of solvent into nonsolvent, PLGA with immobilized AgNpPGA and ascorbic acid precipitates, and the solution becomes whitish. This was followed by addition (stabilization) of the obtained suspension PLGA/AgNpPGA/AscH dropwise into 45 mL of PVP (0.05 wt %). The reactions were conducted at room temperature and ambient pressure. The content of AgNpPGA/AscH was adjusted to produce particles with PLGA/AgNpPGA/AscH ratio of 80/5/15 wt %. Previously we have shown that the optimal PLGA/AscH ratio for retaining sphericity of the particles is 85/15 per weight.[19,20] The resulting emulsion was stirred to allow the organic solvent to evaporate and subsequently poured into a Petri dish and placed into a freezer for overnight incubation. Freeze-drying, a.k.a., lyophilization, was utilized at −57 °C and the pressure of 0.3 mbar. The main drying was performed at −57 °C for 8.5 h, and the final drying was done for 30 min at −30 °C using Freeze Dryer Martin Christ Alpha 1-2/LD plus. The encapsulation efficiency (EE %) was found to be more than 90%.

An integrated study of the nanosphere composition and structure was carried out by combining different techniques, i.e., by XRD analysis, field emission scanning electron microscopy (FE-SEM), and dynamic light scattering (DLS). The more details regarding characterization of the samples are provided within the SI.

The effect of different amounts of samples, blank PLGA particles, or PLGA/AgNpPGA/AscH nanoparticles, on the basal level of intracellular superoxide, was measured using a fluorescent sensor for superoxide, hydroethidine (Invitrogen). Human umbilical vein cells (HUVECs) were used, and intracellular superoxide formation was detected with hydroethidine (HE). Cells were incubated with 5 uM HE

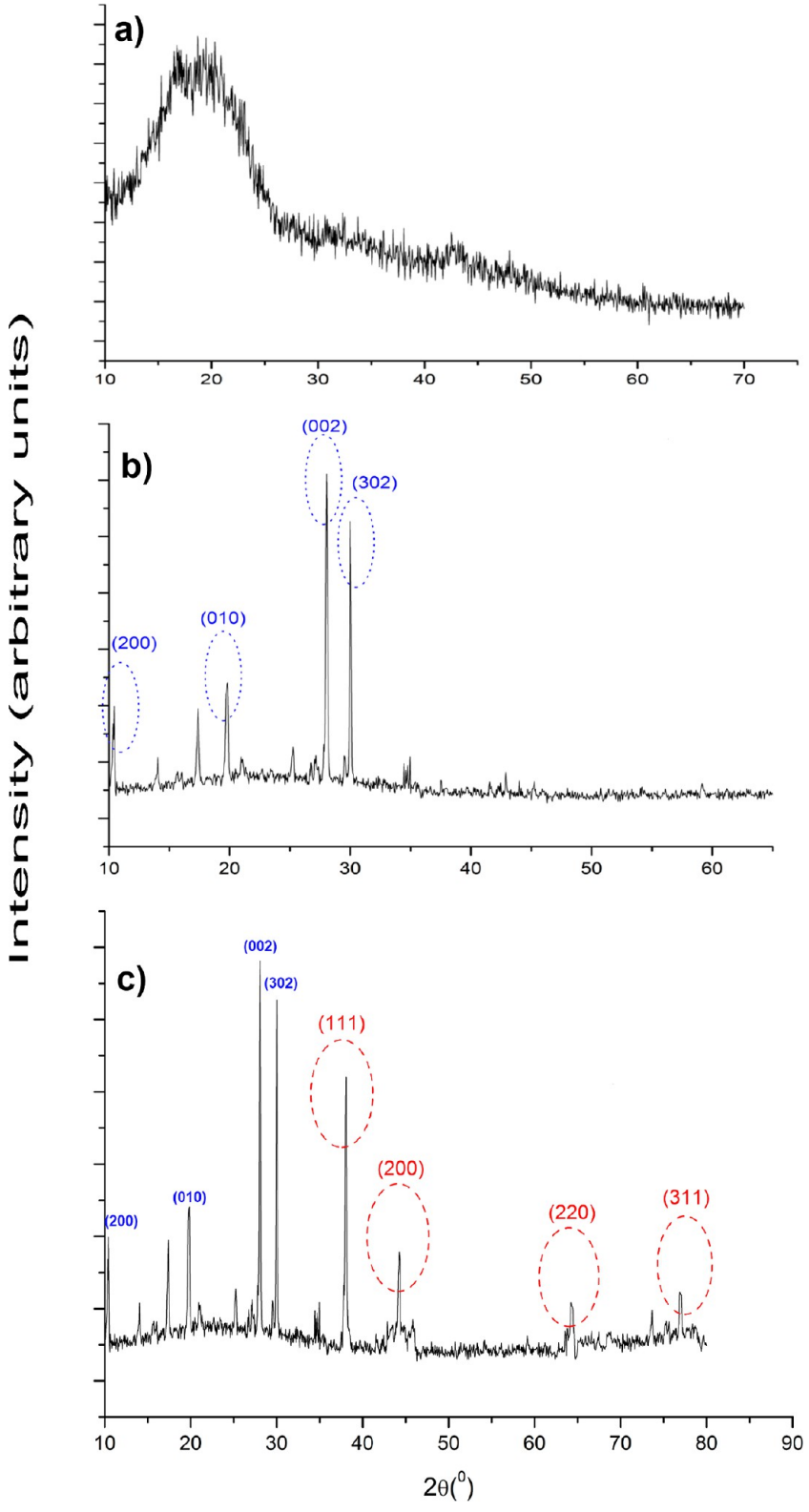

Figure 2. XRD diffraction patterns of (a) PLGA, (b) PLGA/AscH, and (c) PLGA/AgNpPGA/AscH.

for 10 min and further processed as previously described[21] and as explained within the SI.

The influence of PLGA/AgNpPGA/AscH nanoparticles on the HUVECs growth and viability was determined by the mitochondrial-dependent reduction of MTT (3-(4,5-dimethylthiazol-2-yl)-2,5-diphenyltetrazolium bromide) to formazan, as formerly reported[22] and described in the SI.

The protocol for the determination of the effect of samples on MC3T3-E1 osteoblastic cells in vitro was performed as described previously[23,24] with modifications and as provided within the SI.

The antibacterial activity of released AgNpPGA/ascorbic acid from PLGA/AgNpPGA/AscH nanospheres was evaluated against Gram-positive bacterium, methicillin-resistant *Staphylococcus aureus* (MRSA; ATCC 43300), and Gram-negative bacterium *Escherichia coli* (ATCC

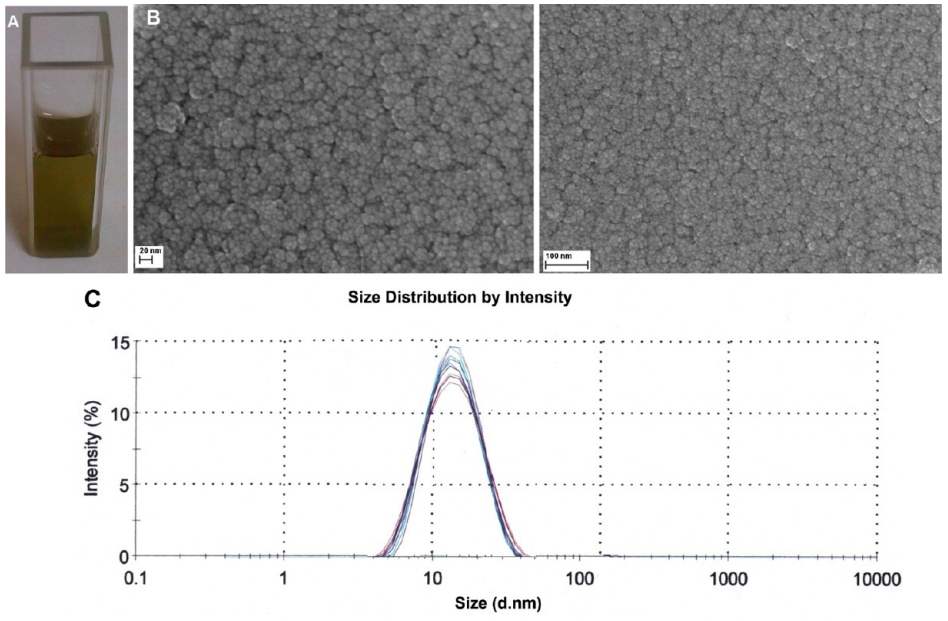

Figure 3. (A) Digital photo showing the yellow-green solution containing silver nanoparticles. (B) Representative FESEM micrographs of silver nanoparticles coated by PGA (AgNpPGAs) (bar 20 nm and 100 nm). (C) Particle size distribution of AgNpPGAs.

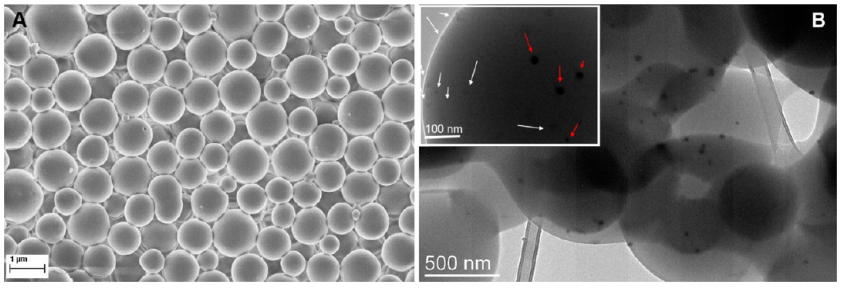

Figure 4. Representative FESEM (A, bar = 1 μm) and TEM (B) images of PLGA/AgNpPGA/AscH particles dried at room temperature and prepared using identical parameters as for freeze-dried formulation. The micrographs are given for comparison purposes. In the TEM micrograph (inset on B) it may be seen that some particles are brighter and some darker, i.e., that AgNpPGAs and ascorbic acid have a different contrast.

25922). The antibacterial activity was evaluated by the broth microdilution method, and MICs were determined following the guidelines of a CLSI.[25]The procedure for the evaluation of the antibacterial activity is also given in the SI.

RESULTS AND DISCUSSION

XRD Analysis. XRD diffraction was used for the phase composition analysis of PLGA/AgNpPGA/AscH particles. No crystalline peaks of the poly(lactide-co-glycolide) have been observed, suggesting its amorphous nature (Figure 2a). The characteristic reflections of ascorbic acid, (002) at 2Θ = 28.0, ($\bar{3}$02) at 2Θ = 29.9, (200) at 2Θ =10.4, (010) at 2Θ = 19.8 (according to ICDD 04-0308),[26] appeared after its encapsulation in PLGA nanospheres (Figure 2(b)). This indicates that AscH was successfully encapsulated by PLGA particles. The XRD analysis led to confirmation of the silver phase, with characteristic strong Bragg reflections corresponding to (111), (200), (220), and (311) planes of fcc silver (JCPDS No.4-0783).[27,28] It indicates the silver nanoparticles were incorporated too within the PLGA particles.

Morphology Studies. PGA, a hydrophilic anionic polyelectrolyte, was employed as capping agent to prevent agglomeration of the AgNps as well as to make them be more biocompatible. As-prepared AgNpPGAs were stable in sols over prolonged periods of time, with no sign of phase separation (Figure 3a). Figure 3b shows representative FESEM images of as-prepared PGA-capped Ag nanoparticles. From these images it can be seen that AgNpPGAs had nearly spherical shapes. The synthesized AgNpPGAs were uniform, with a narrow particle size distribution and mean size of about 5 nm. Larger AgNpPGAs with sizes of about 15−30 nm were clusters of the smaller Ag nanoparticles. Measurements of the particle size distribution based on DLS showed that 10% of particles were 5 nm in diameter; 50% of particles had diameters of less than 21 nm, while 90% of particles were of diameters below 45 nm (Figure 3c).

Without liophilization, PLGA/AgNpPGA/AscH particles prepared by the physicochemical solvent/nonsolvent method and by drying at room temperature had a similarly narrow size distribution but were micrometer-sized (Figure 4). Figure 4 shows spherical particles with a smooth surface.

Freeze-dried PLGA/AgNpPGA/AscH particles were analyzed by FESEM and by DLS to study their morphology and to quantify the particle size. PLGA/AgNpPGA/AscH particles were uniform and spherical and had a smooth and regular surface (Figure 5A). A size distribution curve for PLGA/AgNpPGA/AscH particles is presented in Figure 3B. The results showed that 10% of the particles were 86 nm in diameter; 50% of particles had

dx.doi.org/10.1021/am402237g | ACS Appl. Mater. Interfaces 2013, 5, 9034−9042

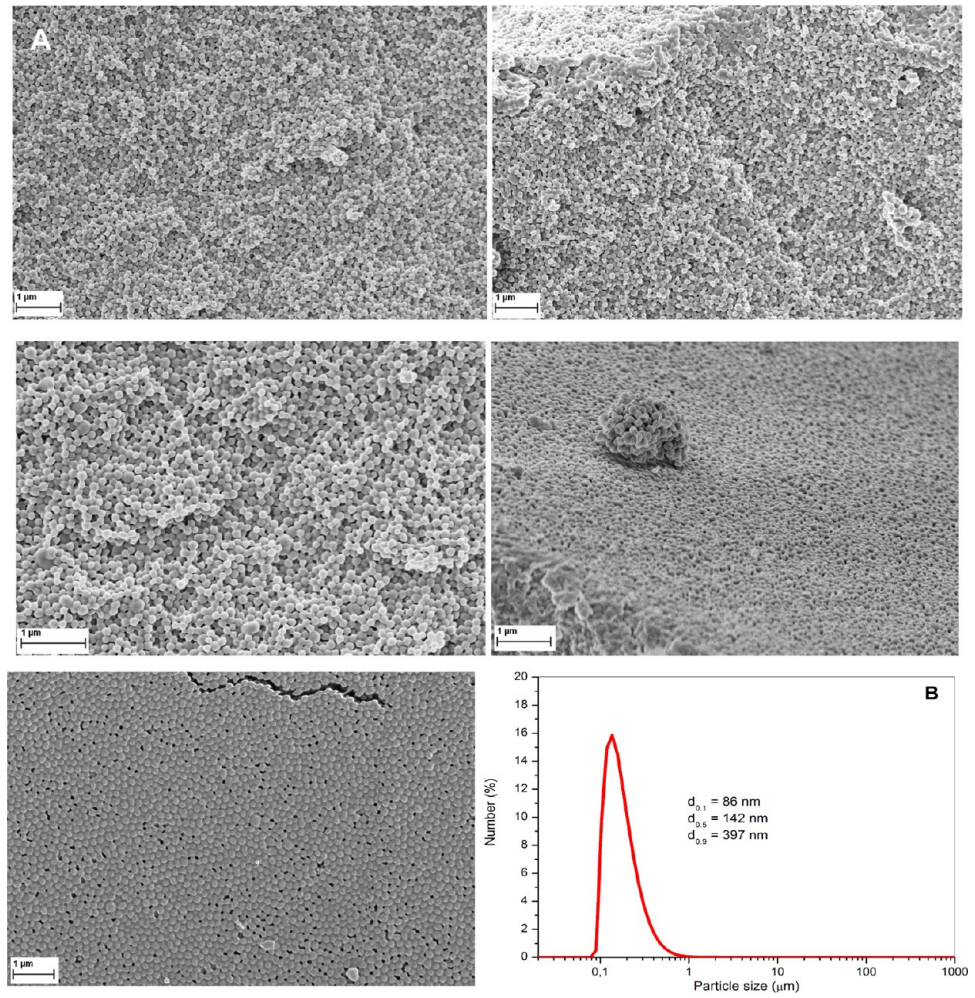

Figure 5. (A) Representative FESEM images of freeze-dried PLGA/AgNpPGA/AscH particles (bar 1 μm) and (B) particle size distribution of PLGA/AgNpPGA/AscH particles.

diameters of less than 142 nm, while 90% of particles were of diameters below 397 nm (Figure 5B). The physicochemical solvent/nonsolvent method is based on the solvent (acetone) diffusion into nonsolvent (ethanol), which results in a fast precipitation and phase separation of the PLGA polymer. After the solvent evaporation and partial freezing in the freezer, the process of freeze drying has been utilized. During the lyophilization, a very important parameter, the product's temperature, cannot be directly controlled. However, parameters such as ambient and condensation temperatures, chamber pressure, duration of lyophilization, the type of cryoprotectant, etc., can be controlled, and these parameters were adjusted to obtain uniformly spherical particles on the nanometre scale. PVP, used in our experiment as a stabilizer for PLGA particles, also served as cryoprotectant during lyophilization of these particles. Also, the optimal duration of lyophilization turned out to be 9 h. PLGA/AgNpPGA/AscH particles generated by the physico-chemical solvent/nonsolvent method and freeze drying had smaller sizes than particles dried at room temperature (Figure 4 and Figure 5). The submicrometer size of the nanoparticles is associated with countless advantages over their microparticulate counterparts. In general, they have a higher intracellular uptake efficiency compared to microparticles. For example, 100 nm sized nanoparticles exhibited 2.5-fold greater uptake when compared to 1 μm sized particles and 6 times higher uptake when compared to 10 μm sized microparticles.[29]

The zeta potential of the PLGA/AgNpPGA/AscH particles remained unchanged, with zeta potential value of −30.2 ±10.5 mV in the pH range 4.3−4.5, before and after freeze-drying.

Detection of Superoxide and MTT Assay. In our previous work and prior to those experiments of detection of superoxide, the influence of the samples AgNp, AgNpPGAs, and PLGA/AgNpPGAs[17] and additionally of PLGA/AgNpPGA/AscH nanoparticles on the production of the reactive oxygen species within cells was determined by dichloro-dihydro-fluorescein diacetate (DCFH-DA) assay,[30] with minor modifications.[31] The protocol was performed as described previously.[31,17] The data from ROS study of prepared PLGA/AgNpPGAs and PLGA/AgNpPGA/AscH nanoparticles were provided in the Supporting Information (SI) as Figure S1. A study on oxidative stress induced in the human hepatoma cell line (Hep G2 cells) confirmed PLGA/AgNpPGAs does not cause generation of intracellular reactive oxygen species (Figure S1b, SI). Moreover, there was reduction of DCF fluorescence in comparison to the controls, for the PLGA with encapsulated AgNpPGAs at 0.1% (Figure S1b, SI). One possible explanation is, as Arora et al. demonstrated in vitro in rat fibroblasts and liver cells, that lower doses of silver nanoparticles can elicit a protective effect against the oxidative stress via a decrease in lipid peroxidation and, at the

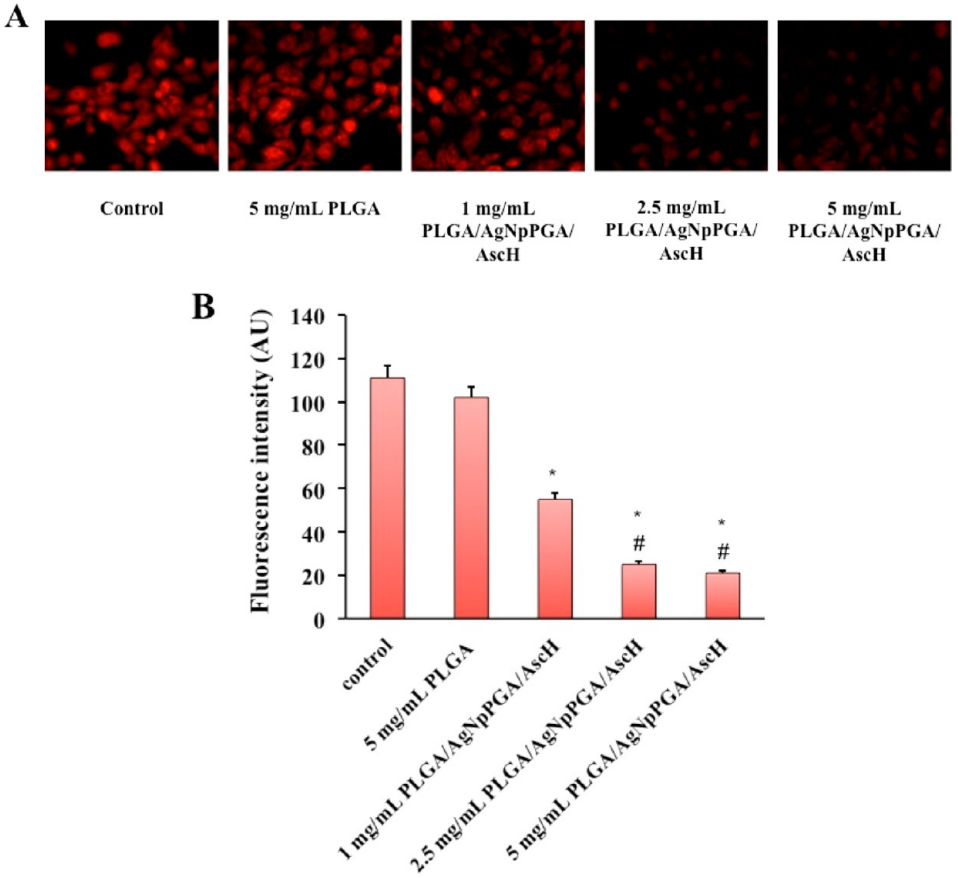

Figure 6. Detection of superoxide in HUVECs subjected to PLGA/AgNpPGA/AscH nanoparticles. (A) Representative fluorescent microscopy images of the HUVECs preloaded with hydroethidine, a superoxide sensitive fluorescent sensor, and then treated with either 5 mg/mL of PLGA or 1, 2.5, and 5 mg/mL of PLGA/AgNpPGA/AscH nanoparticles for 45 min. (B) Intensity of fluorescence determined from the experiment shown in (A). $n = 50-100$ cells; $^*p < 0.001$ compared to the control, # $p < 0.001$ compared to the effect of 1 mg/mL of PLGA/AgNpPGA/AscH nanoparticles.

same time, an increase in glutathione transferase and superoxide dismutase production, the two species that play a critical role in decomposing ROS in organisms.[32] Another possibility is that PLGA has a protective role against oxidative stress-induced cell death. According to Reddy and collaborators, PLGA nanoparticles protected in vitro culture of human fetal neurons against oxidative stress challenged with hydrogen peroxide.[33] However, we have obtained even more interesting results in the case of PLGA/AgNpPGA/AscH nanoparticles which at concentrations of 0.01, 0.1, and 1% (v/v) caused a significant decrease in DCF fluorescence, which was after 5 h exposure 2-fold lower than that in control cells (Figure S1a, SI). This indicates that PLGA/AgNpPGA/AcsH nanoparticles either act as scavengers of intracellular reactive oxygen species and/or reduce their formation.

To further verify and confirm these results, we have tested the ability of blank PLGA and PLGA/AgNpPGA/AscH nanoparticles to scavenge a superoxide anion radical.

The superoxide anion radical ($O_2^{\bullet -}$) is a one-electron-reduced byproduct of respiration that is considered to be a constituent of reactive oxygen species (ROS).[34] Normally produced by mitochondria, superoxide is detoxified by the class of enzymes called superoxide dismutases (SOD).[34] However, with aging and in different pathologies, such as inflammation-based diseases, the amount of produced $O_2^{\bullet -}$ increases or/and the activity of the SOD enzyme decreases, leading to oxidative stress and tissue damage.[35] Ascorbate is known to scavenge ROS and prevent oxidative stress.[36] We have thus tested the ability of blank PLGA and PLGA/AgNpPGA/AscH nanoparticles to scavenge superoxide that is produced by the mitochondrial electron transport chain.

First, the effect of PLGA/AgNpPGA/AscH nanoparticles on cell growth was tested by MTT assay. No significant changes on cell proliferation were observed in the first 24 h of incubation with 1, 2.5, and 5 mg/mL of PLGA/AgNpPGA/AscH nanoparticles (data not shown), suggesting that neither the carrier nor the coated particles is toxic for the cells in the used concentration range.

Next, hydroethidine (HE) loaded HUVECs were incubated for 45 min with the same concentration range of PLGA/AgNpPGA/AscH nanoparticles and 5 mg/mL of blank PLGA. The characteristic fluorescence of 2-hydroxyethidium, which is the product of the reaction of HE with superoxide, was then observed by fluorescence microscopy (Figure 6A) and semi-quantified (Figure 6B) using ImageJ (NIH) software. As shown in Figure 6, superoxide was detected in untreated HUVECs as a consequence of the normal respiration process. Treatment with the highest dose of blank PLGA did not induce any considerable change in the amount of intracellular superoxide. However, treatment with only 1 mg/mL of PLGA/AgNpPGA/AscH nanoparticles halved the intracellular level of superoxide. The doses of 2.5 and 5 mg/mL almost completely abolished the intracellularly produced superoxide. These data demonstrate that PLGA/AgNpPGA/AscH nanoparticles appeared to be capable of efficiently delivering ascorbate to the cells, which could have an immense therapeutic potential in preventing oxidative stress.

dx.doi.org/10.1021/am402237g | ACS Appl. Mater. Interfaces 2013, 5, 9034−9042

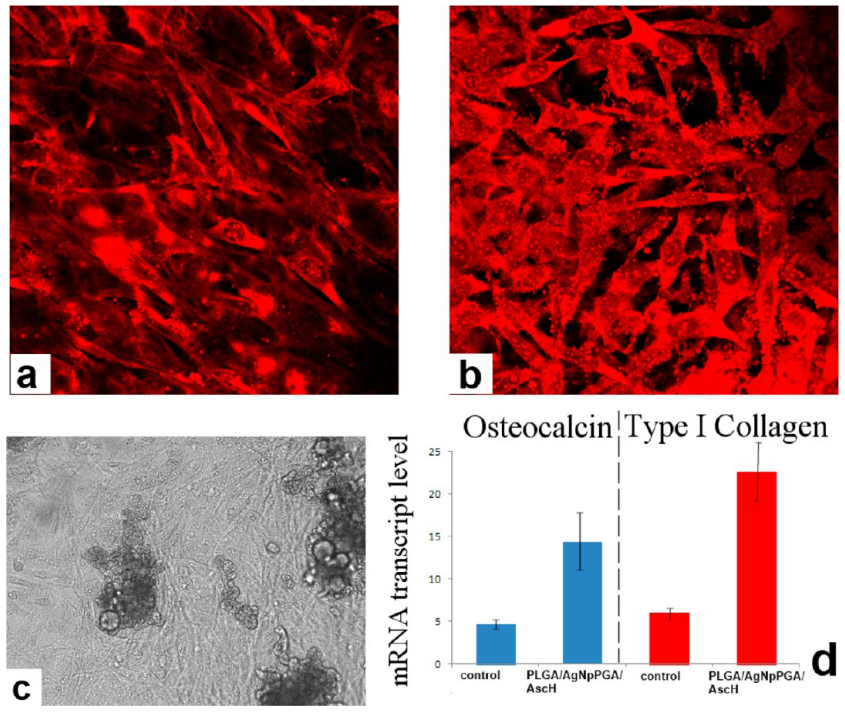

Figure 7. Effect of PLGA/AgNpPGA/AscH samples on MC3T3-E1 osteoblastic cells in vitro. (a, b) Single plane confocal optical images of fluorescently counterstained osteoblastic MC3T3-E1 cells (red) after 7 days of incubation in differentiation medium: (a) control; (b) PLGA/AgNpPGA/AscH. (c) Optical micrographs showing the interface between the osteoblastic MC3T3-E1 cells and conglomerates of PLGA/AgNpPGA/AscH particles. Magnifications: 60× (a, b); 20× (c). (d) The effect of PLGA/AgNpPGA/AscH particles on the mRNA expression of osteocalcin and type I procollagen in osteoblastic MC3T3-E1 cells. mRNA expression was quantified by quantitative RT-polymerase chain reaction relative to the housekeeping gene, β-actin. Data normalized to expression of β-actin are presented as arithmetic means with error bars representing standard deviation. Both genes were significantly ($p < 0.05$) upregulated with respect to the control group.

The cellular uptake of vitamin C is somewhat limited by the fact that cells more efficiently take dehydroascorbate than vitamin C, which in turn has to be reduced back to ascorbate.[32] Our data suggest that pharmacologically efficient amounts of vitamin C could be easily achieved by the use of PLGA/AgNpPGA/AscH nanoparticles.

Effect of PLGA/AgNpPGA/AscH Particles on MC3T3-E1 Osteoblastic Cells in Vitro. Results of the investigation of the effect of PLGA/AgNpPGA/AscH nanoparticles on MC3T3-E1 osteoblastic cells in culture are shown in Figure 7. Figure 7a,b displays the confocal optical images of fluorescently counterstained osteoblastic cells of the control sample (Figure 7a) and following incubation with the ascorbic-acid-containing particles prepared within this study (Figure 7b). The cells appear to be spread well on the glass surface, and no patches of dying or morphologically unhealthy cells were observed, suggesting a viable response of the cells to the material. The light microscopy image shown in Figure 7c demonstrates the direct contact established between the nanoparticles and the cells, suggesting furthermore the cells' attraction to the particles, a good indicator of their osteoconductivity. Finally, as shown in Figure 7d, the gene expression of two major osteogenic markers, osteocalcin and type I procollagen, was markedly more upregulated compared to the control: 3-fold for osteocalcin and more than 4-fold for type I procollagen. One possible explanation is that ascorbic acid is required for the differentiation of MC3T3-E1 fibroblasts to osteoblasts. Ascorbic acid was, for example, shown to drastically increase the expression of alkaline phosphatase and osteocalcin.[37] With the additional supplementation of this compound to the cells, their osteoblastic markers become further expressed. Ascorbic acid is also involved in the formation of collagen,[38] which may explain the boosted expression of the gene encoding for its main precursor, type I procollagen, following the treatment with the particles loaded with ascorbic acid.

Biomaterials for bone engineering applications are usually divided into three categories: osteoconductive, osteoinductive, and osteogenic.[39] While osteoconductive materials are conducive to new bone growth on their surface, the osteoinductive ones are able to induce recruitment, differentiation, and proliferation of bone cells, and the osteogenic ones are, according to the standard definition, internally enriched with osteoprogenitor cells, undifferentiated mesenchymal stem cells, or cells already differentiated into the osteoblastic lineage. The osteoinductive nature of PLGA/AgNpPGA/AscH nanoparticles is evidenced hereby by their ability to upregulate the expression of osteocalcin and type I procollagen in osteoblastic MC3T3-E1 cells.

Antibacterial Activity. β-Lactams represent the cornerstones of conventional anti-infective therapies.[40] Their central downside comes from the fact that the clinical application of β-lactams can result in the increased prevalence and virulence of the bacterial strains targeted by the therapy. The exploration of venues that would lead to alternative antibacterial therapies consequently presents one of the central challenges posed before modern medicine.[41,42]

To assess the antibacterial activity of released AgNpPGA, samples were tested against Gram-positive *Staphylococcus aureus* (MRSA) and Gram-negative *Escherichia coli* (Figure 8 and Figure S2 in the enclosed SI). We evaluated the release media from an early time point in the experiment, day 2, as well as later time points, days 28, 59, and 82 (Figure 8), and the MICs of the tested compounds were determined. The data demonstrate that the

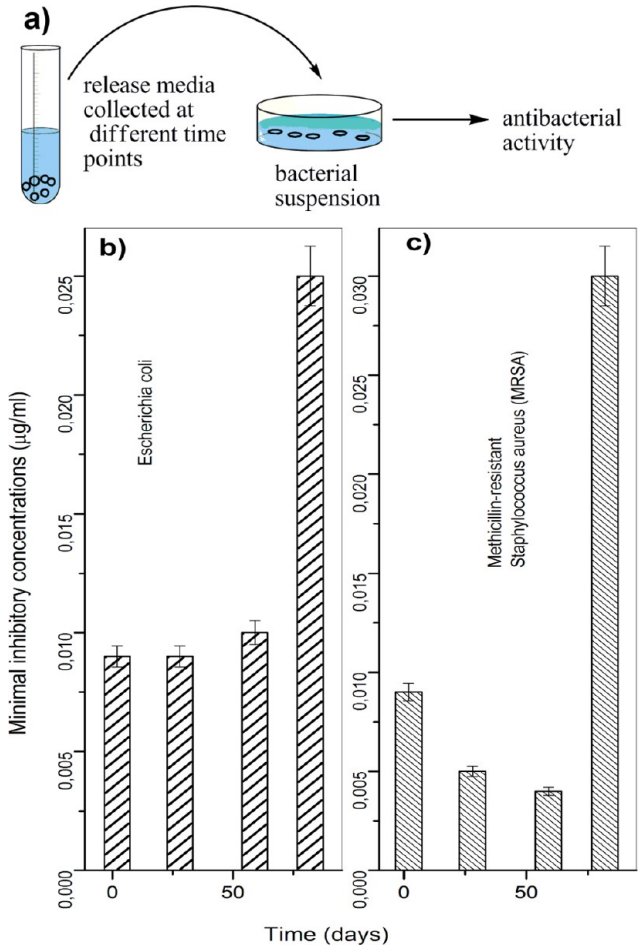

Figure 8. Antibacterial activity of PGA-capped silver nanoparticles released from freeze-dried PLGA/AgNpPGA/AscH. (a) Schematic of the experiment. (b,c) Minimal inhibitory concentrations of AgNpPGAs determined using a broth microdilution assay as a function of time, against *E. coli* (b) and MRSA (c).

media containing released silver exhibit strong antibacterial activity against *S. aureus* as well as *E. coli*, with the media collected at 28 and 59 day time points being even more antibacterially active in the case of *S. aureus* than media which contained initially released silver. In the case of *E. coli*, the MIC remained almost the same up to 59 days followed by an increase at the 82 day time point. A similar increase in the MIC also occurred in the case of *S. aureus* at day 82. The different behavior and MICs between the two bacterial strains up to 59 days can be explained by assuming that at the given concentration of AgNps the growth inhibition depends on the initial number of cells.[43] On the other side, the possible explanation of such similar behavior at 82 day might be that silver nanoparticles at the later time points are more agglomerated, thus creating clusters which pose lesser antibacterial activity. This is in line with the previously reported findings.[40] One of them is that the small size of the particles facilitates their penetration across the cell membrane and endows them with the ability to affect the intracellular processes. Additionally, tremendous antibacterial properties exhibited by silver nanoparticles are owing to their large surface, which allows for a maximum contact with the local environment,[44] and positive surface charge, which makes their penetration of the negatively charged cell membrane even more facile. It has been known that silver nanoparticles are capable of penetrating the bacterial cell wall and imposing irretrievable damage on it and ultimately causing the death of the organism.[45] In addition, ascorbic acid was found to be effective in treating wound infection by interfering with the colony formation of microorganisms.[46,47] Also, lactic acid, one of the products of the PLGA degradation, is widely employed for controlling microbial growth which is associated with the pH lowering effect.[48] In one form or another, silver and its compounds have long been used as antimicrobial agents. Understanding the antimicrobial mechanism of nanoparticle formulations is important for the sake of creating an optimal synergy with biomolecules. To gain a better insight into the mechanism of action of silver nanoparticles as bactericidal as well as antifungal or antiviral agents, further examination of the membrane-bound and intracellular nanoparticles[45]will be needed.

CONCLUSION

In this study, a simple, combined freeze-drying method and physicochemical solvent/nonsolvent approach to preparation of multifunctional PLGA nanospheres encapsulating AgNpPGAs and ascorbic acid is demonstrated. Freeze-dried PLGA/AgNpPGA/AscH particles were uniform, spherical, and with the mean diameter of 142 nm. PLGA/AgNpPGA/AscH nanoparticles appeared to be capable of efficiently delivering ascorbate to the cells, which could have a tremendous therapeutic potential in preventing oxidative stress. The given particles also had a positive effect on MC3T3-E1 osteoblastic cells in vitro. They promoted an intimate contact with osteoblastic cells and preserved their healthy morphologies, without reducing the cell viability. PLGA/AgNpPGA/AscH nanoparticles showed multiple-fold upregulation of two osteogenic markers: osteocalcin and type I procollagen. In addition, PLGA/AgNpPGA/AscH nanospheres prepared in this study showed superior and extended antibacterial activity against Gram-positive methicillin-resistant *Staphylococcus aureus* and Gram-negative *Escherichia coli*, the main causative agents of orthopedic infections.

From the perspective of materials and device development, PLGA/AgNpPGA/AscH particles exhibited strong bactericidal, antioxidative, and osteoinductive properties, making them a promising candidate for application in the clinic, especially in orthopedic surgery.

ASSOCIATED CONTENT

Supporting Information

Experimental procedures: Chemicals for the synthesis of freeze-dried PLGA/AgNpPGA/AscH nanospheres; Preparation of PGA-capped silver nanoparticles; Characterization of the samples; Detection of superoxide; Determination of the effect of PLGA/AgNpPGA/AscH nanoparticles on the cell growth and viability by MTT assay; Determination of the effect of PLGA/AgNpPGA/AscH particles on MC3T3-E1 osteoblastic cells in vitro; Antibacterial activities and determination of minimal inhibitory concentrations; Figure S1: PLGA/AgNpPGA/ascorbic-acid nanoparticles (a) and PLGA/AgNpPGA particles (b) - induced intracellular reactive oxygen species formation in human hepatoma cells (HepG2) cells. Figure S2: Representative microplate wells for antibacterial activity. The darker color implies bacterial viability is more pronounced, MRSA (a) and *E. coli* (b). We tested release media after 2 (A), 28 (B), 59 (C), and 82 days (D). This material is available free of charge via the Internet at http://pubs.acs.org.

AUTHOR INFORMATION

Corresponding Author

*E-mail: magdalena.stevanovic@itn.sanu.ac.rs; magir@eunet.rs.

Notes

The authors declare no competing financial interest.

ACKNOWLEDGMENTS

This research was supported by the Ministry of Education, Science and Technological Development of the Republic of Serbia, under Grant No. III45004. Presented were the results of a study supported by the NIH/NIDCR grant K99-DE021416. Confocal microscopy data for this study were acquired at the Nikon Imaging Center at UCSF. M.R.F. acknowledges the intramural support from the University of Erlangen-Nuremberg within Emerging Field Initiative (EFi-MRIC). The authors are thankful to Marina Milenković for the examination of antibacterial activity, Miodrag Mitrić for the XRD analysis, and Mirjana Marković for the determinations of zeta potential.

REFERENCES

(1) Haley, R. W.; Culver, D. H.; White, J. W.; Morgan, W. M.; Emori, T. G.; Munn, V. P.; Hooton, T. M. *Am. J. Epidemiol.* **1985**, *121*, 182−205.

(2) Bouza, E.; Burillo, A.; Munoz, P.; Guinea, J.; Marin, M.; Rodriguez-Creixems, M. *J. Antimicrob. Chemother.* **2013**, *68*, 1881−1888.

(3) Muller, A. E.; Punt, N.; Mouton, J. W. *J. Antimicrob. Chemother.* **2012**, *68*, 900−906.

(4) McGeer, A.; Campbell, B.; Emori, T. G.; Hierholzer, W. J.; Jackson, M. M.; Nicolle, L. E.; Peppier, C.; Rivera, A.; Schollenberger, D. G.; Simor, A. E.; Smith, P. W.; Wang, E. E.-L. *Am. J. Infect. Control.* **1991**, *19*, 1−7.

(5) Cruse, P. J.; Foord, R. *Surg. Clin. North Am.* **1980**, *60*, 27−40.

(6) Nel, A. E.; Mädler, L.; Velegol, D.; Xia, T.; Hoek, E. M. V.; Somasundaran, P.; Klaessig, F.; Castranova, V.; Thompson, M. *Nat. Mater.* **2009**, *8*, 543−557.

(7) Mahmoudi, M.; Serpooshan, V. *ACS Nano* **2012**, *6*, 2656−2664.

(8) Valko, M.; Rhodes, C. J.; Moncol, J.; Izakovic, M.; Mazur, M. *Chem.-Biol. Interact.* **2006**, *160*, 1−40.

(9) Lewinski, N.; Colvin, V.; Drezedk, R. *Small* **2008**, *4*, 26−49.

(10) Auten, R. L.; Davis, J. M. *Pediatr. Res.* **2009**, *66*, 121−127.

(11) Kratz, F.; Warnecke, A. *J. Controlled Release* **2012**, *164*, 221−235.

(12) Jain, S.; Rathi, V. V.; Jain, A. K.; Das, M.; Godugu, C. *Nanomedicine* **2012**, *7*, 1311−1337.

(13) Patel, N. R.; Damann, K.; Leonardi, C.; Sabliov, C. M. *Nanomedicine* **2011**, *6*, 1381−1395.

(14) Puppi, D.; Chiellini, F.; Piras, A. M.; Chiellini, E. *Prog. Polym. Sci.* **2010**, *35*, 403−440.

(15) Danhier, F.; Ansorena, E.; Silva, J. M.; Coco, R.; Le Breton, A.; Préat, V. *J. Controlled Release* **2012**, *161*, 505−522.

(16) Stevanović, M.; Savanović, I.; Uskoković, V.; Škapin, S. D.; Bračko, I.; Jovanović, U.; Uskoković, D. *Colloid Polym. Sci.* **2012**, *290*, 221−231.

(17) Stevanovic, M.; Škapin, S. D.; Bračko, I.; Milenković, M.; Petković, J.; Filipič, M.; Uskoković, D. *Polymer* **2012**, *53*, 2818−2828.

(18) Stevanović, M.; Kovačević, B.; Petković, J.; Filipič, M.; Uskoković, D. *Int. J. Nanomed.* **2011**, *6*, 2837−2847.

(19) Stevanović, M.; Savić, J.; Jordović, B.; Uskoković, D. *Colloids Surf., B* **2007**, *59*, 215−223.

(20) Stevanović, M.; Maksin, T.; Petković, J.; Filipic, M.; Uskoković, D. *Nanotechnology* **2009**, *20*, 335102.

(21) Filipovic, M. R.; Miljkovic, J. Lj.; Nauser, T.; Royzen, M.; Klos, K.; Shubina, T.; Koppenol, W. H.; Lippard, S. J.; Ivanović-Burmazović, I. *J. Am. Chem. Soc.* **2012**, *134*, 12016−12027.

(22) Filipović, M. R.; Koh, A. C. W.; Arbault, S.; Niketic, V.; Debus, A.; Schleicher, U.; Bogdan, C.; Guille, M.; Lemaître, F.; Amatore, C.; Ivanović-Burmazović, I. *Angew. Chem., Int. Ed. Engl.* **2010**, *49*, 4228−4232.

(23) Ignjatović, N.; Uskoković, V.; Ajduković, Z.; Uskoković, D. *Mater. Sci. Eng., C* **2013**, *33*, 943−950.

(24) Uskoković, V.; Desai, T. A. *J. Biomed. Mater. Res. A* **2013**, *101*, 1427−1436.

(25) Clinical and Laboratory Standards Institute (CLSI): Performance Standards for Antimicrobial Susceptibility Testing: 15th Informational Supplement. CLSI Document M100-S15. Wayne, PA, USA; 2005.

(26) ICDD file No. 04-0308 (Ascorbic acid), International Center for Diffraction Data.

(27) Pragatheeswaran, A.; Kareem, T. A.; Kaliani, A. A. *J. Phys. Conf. Ser.* **2010**, *208*, 012109.

(28) Powder diffraction files (International Centre for Diffraction Data): JCPDS card numbers 41-1402 and 04-0783.

(29) Abdelwahed, W.; Degobert, G.; Stainmesse, S.; Fessi, H. *Adv. Drug Delivery Rev.* **2006**, *58*, 1688−1713.

(30) Osseni, R.; Debbasch, C.; Christen, M. O.; Rat, P.; Warnet, J. M. *Toxicol. In Vitro* **1999**, *13*, 683−688.

(31) Petković, J.; Žegura, B.; Stevanović, M.; Drnovšek, N.; Uskoković, D.; Novak, S.; Filipič, M. *Nanotoxicology* **2011**, *5*, 341−353.

(32) Arora, S.; Jain, J.; Rajwade, J. M.; Paknikar, K. M. *Toxicol. Lett.* **2008**, *179*, 93−100.

(33) Reddy, M. K.; Wu, L.; Kou, W.; Ghorpade, A.; Labhasetwar, V. *Appl. Biochem. Biotechnol.* **2008**, *151*, 565−577.

(34) Ivanović-Burmazović, I.; Filipović, M. R. *Adv. Inorg. Chem.* **2012**, *64*, 53−95.

(35) Cuzzocrea, S.; Riley, D. P.; Caputi, A. P.; Salvemini, D. *Pharmacol. Rev.* **2001**, *53*, 135−159.

(36) Dhar-Mascareño, M.; Cárcamo, J. M.; Golde, D. W. *Free Radical Biol. Med.* **2005**, *38*, 1311−1322.

(37) Francesci, R. T.; Iyer, B. S.; Cui, Y. J. *Bone Miner. Res.* **1994**, *9*, 843−54.

(38) Murad, S.; Grove, D.; Lindberg, K. A.; Sivarajah, A.; Pinnell, S. R. *Proc. Natl. Acad. Sci. U.S.A.* **1981**, *78*, 2879−2882.

(39) Mistry, A. S.; Mikos, A. G. *Adv. Biochem. Eng./Biotechnol.* **2005**, *94*, 1−22.

(40) Master, R. N.; Deane, J.; Opiela, C.; Sahm, D. F. *Ann. N. Y. Acad. Sci.* **2013**, *1277*, 1−7.

(41) Riccio, D.A.; Coneski, P. N.; Nichols, S. P.; Broadnax, A. D.; Schoenfisch Mark, H. *ACS Appl. Mater. Interfaces* **2012**, *4*, 796−804.

(42) Uskoković, V.; Batarni, S. S.; Schweicher, J.; King, A.; Desai, T. A. *ACS Appl. Mater. Interfaces* **2013**, *5*, 2422−2431.

(43) Sukdeb, P.; Yu, K. T.; Joon, M. S. *Appl. Environ. Microbiol.* **2007**, *73*, 1712−1720.

(44) Krutyakov, Y. A.; Kudrinskiy, A.; Yu Olenin, A.; Lisichkin, G. V. *Russ. Chem. Rev.* **2008**, *77*, 233−257.

(45) Ravindran, A.; Chandran, P.; Khan, S. S. *Colloids Surf., B* **2013**, *105*, 342−352.

(46) Nagoba, B. S.; Wadher, B. J.; Selkar, S. P. *J. Anim. Vet. Adv.* **2011**, *3*, 26−28.

(47) Mujumdar, R. K. *Indian J. Surg.* **1993**, *55*, 501−507.

(48) Radovic-Moreno, A. F.; Lu, T. K.; Puscasu, V. A.; Yoon, C. J.; Langer, R.; Farokhzad, O. C. *ACS Nano* **2012**, *6*, 4279−4287.